International Journal of Modern Physics E
Vol. 21, No. 7 (2012) 1250066 (13 pages)

DOI: 10.1142/S0218301312500668

World Scientific
www.worldscientific.com

STRUCTURE OF TWO-NEUTRON HALO NUCLEI, ^{11}Li

WALEED S. HWASH*,†,‡, REDZUWAN YAHAYA*,
SHAHIDAN RADIMAN* and AZNAN FAZLI ISMAIL*

*School of Applied Physics, Faculty of Science and Technology,
Universiti Kebangsaan Malaysia, 43600 Bangi, Selangor, Malaysia
†Department of Physics, Faculty of Education for Pure Sciences,
Anbar University, Anbar, Iraq
‡waleed973@yahoo.com

Received 14 February 2012
Revised 29 May 2012
Accepted 29 May 2012
Published 19 June 2012

The two-neutron halo nucleus ^{11}Li has been investigated in this work. Jacobi coordinates is used to describe the three-body system, using two configurations that are the T-configuration and Y-configuration. The calculations have been calculated based on a cluster model. The ^{11}Li nucleus is considered as three-body system core (^{9}Li) + n + n. The core here has been considered as a deformed core. The calculations confirmed that the core has some deformation and has an oblate shape which in turn has effects on the structure of three-body system.

Keywords: Nuclear structure; ^{11}Li; cluster model; halo nuclei.

PACS Number(s): 21.45.+v, 21.60gx

1. Introduction

The development of radioactive nuclear beams (RNB) through high-energy fragmentation has proven to be very useful in the study of the nuclear structure of neutron-rich nuclei close to the so-called neutron-drip line, i.e., the threshold for fragmentation into neutrons and other components. It was found in a series of experiments[1–3] on light nuclei that ^{11}Li, ^{14}Be and ^{17}B have an abnormally large root-mean-square (rms) radius. Hansen and Jonson have pointed out[4] that this is due to the neutron halo in the nucleus which gave new implications to the theory of nuclear structure and nuclear reaction. Indeed studies on halo nuclei have attract many nuclear physicists.

In general, the halo phenomenon is a threshold effect occurring in loosely bound systems, in which particles are held in short-range potential wells. In favorable status, a barely trapped particle or particles (or a cluster of particles) may tunnel out

into the classically forbidden region. This "leakage" populates very dilute and fragile structures near particle emission thresholds. The more loosely the halo particles are confined, the more clearly "the halo stratosphere" is developed.[5]

In nuclear physics, the most obvious three-body halo candidates are light dripline nuclei with two neutrons encircling a core. Among them ^{11}Li ($= {}^{9}\text{Li}+n+n$) is a nuclear halo system. The first discovery of ^{11}Li was back in the 1960s.[6] There have been a series of experiments to study ^{11}Li. The interaction cross-section of lithium isotopes colliding with nuclear targets was measured.[7] The abnormally large values for ^{11}Li were soon interpreted as a consequence of extended neutron densities, a neutron halo, consisting of a di-neutron coupled to a ^{9}Li core.[4] This was later supported by a measurement of the momentum distribution of ^{9}Li after the break-up of ^{11}Li.[8] The material presented in this section is based on the paper.[5] In the paper, the value[9] 295 ± 26 keV was used for the two-neutron separation energy in ^{11}Li. However, as also commented in the paper, another experimental value[10] 376 ± 5 keV was reported for the two-neutron separation energy and, this later value was finally corrected to be 378 ± 5 keV.[11] The di-neutron model suggested large two-neutron removal cross-sections *via* Coulomb dissociation. The cross-sections of electromagnetic dissociation of ^{11}Li on high-Z targets at high[12] and low beam energies[13] were found to reach abnormally large values. Later, charge-exchange cross-sections of ^{8,9,11}Li were calculated to be about the same,[14] thus implying that the ^{9}Li core is little disturbed in ^{11}Li. One of the first attempts to indirectly deduce the neutron density of ^{11}Li can be found in Ref. 15. The authors concluded that only density distributions with very long tails consistently reproduce the observed interaction cross-sections. Furthermore, the angular distributions of ^{9}Li and ^{11}Li nuclei scattered elastically from protons are similar, but the elastic scattering cross-section is smaller by about a factor of two for ^{11}Li.[16]

β-decay denotes an interesting alternative for extracting information about halo structure. Experimental efforts in this direction reported in Refs. 17, 18 and recently in Ref. 19 give indication that the β-decay takes place basically in the halo of ^{11}Li, and that it proceeds mainly to the $^{9}\text{Li} + d$ continuum, opening up a new means to study the halo phenomenon in ^{11}Li. The early reaction experiments were extended in later years, see for example reviews in Refs. 20 and 21. They contain transfer, stripping and break-up reaction studies providing differential, rather than integrated cross-sections. Reaction and decay experiments have been accompanied by precise measurements of static properties: Measurements of two-neutron separation energy by methods of radio-frequency spectrometry[22] and Penning trap[23] for ^{11}Li, nuclear charge radius determined by laser spectroscopy for ^{11}Li,[24] and electric quadrupole and magnetic moments of ^{11}Li from nuclear magnetic resonance experiments.[25]

There have been several theoretical studies of this nucleus. The early di-neutron models of ^{11}Li, such as,[4] turned out to be too schematic to quantitatively describe experimental data and were soon followed by more sophisticated three-body approaches. In the first generation, the three-body models of these nuclei treated the

core as a fully inert object. Several methods of treating the three-body problem were applied to ^{11}Li. They include the Faddeev approach,[26–28] the hyperspherical harmonics method,[26,29] the variational method on a harmonic oscillator basis,[30] the two-body Green's function,[31] and the cluster-orbital shell model.[32,33] Some calculations within a pairing model were reported in Ref. 34. In all their generosity, the three-body models of the next generation rewarded the core with some degrees of freedom, namely with rotational modes.[35] The no-core shell model[36] is another sophisticated approach, which as its name suggests, is a shell model with all particles active in harmonic oscillator shells; i.e., there is no inert core like in standard shell model calculations. The model has been applied to ^{11}Li.[37] Somewhere between few-body and truly microscopic models are microscopic cluster models, in which some degrees of freedom are frozen to reduce the computational demands.

This is achieved through the formation of microscopic clusters with a simplified internal structure within the nucleus being modeled. To a certain extent, cluster structures can also be recognized in some of the microscopic models mentioned above. The stochastic variational model[38] and its multi-cluster version[39] has been applied to lithium[40] isotopes. With simpler phenomenological forces of adjusted strength, the model has been able to reproduce basic (three-body-like) properties of ^{11}Li.

2. Theoretical Framework

The three-body system or two-neutron halo nuclei should be defined in terms of core and valence neutrons.

The distances between each pair of particles $\mathbf{r}_{jk}$ and the distance between the center of mass of the pair and the corresponding third particle (represented in Fig. 1), can be expressed in terms of the Jacobian coordinates $(\mathbf{x}, \mathbf{y})$

$$\text{where} \quad x = \sqrt{A_{jk}}\mathbf{r}_{jk} = \sqrt{\frac{A_j A_k}{A_j + A_k}}\mathbf{r}_{jk}$$

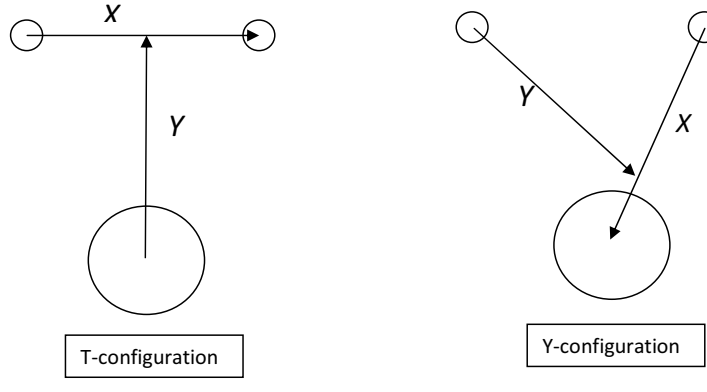

Fig. 1. Jacobi coordinates for three-body system.

$$\text{and} \quad y_i = \sqrt{A_{(jk)i}}\mathbf{r}_{(jk)i} = \sqrt{\frac{(A_jA_k)A_i}{A_i + A_j + A_k}}\mathbf{r}_{(jk)i}\,.$$

The intrinsic Hamiltonian of the core determines a set of eigenstates ϕ_{core} and eigenvalues ξ_{core}

$$\text{with} \quad \hat{h}_{\text{core}}(\xi_{\text{core}})\phi_{\text{core}}(\xi_{\text{core}}) = \varepsilon_{\text{core}}\phi_{\text{core}}(\xi_{\text{core}})\,. \tag{1}$$

The total wave function of the system from Jacobi coordinates

$$\Psi^{\text{JM}}(x, y, \boldsymbol{\xi}) = \phi_{\text{core}}(\xi_{\text{core}})\psi(x, y) \tag{2}$$

$\Psi(x, y)$ contains the radial, angular and spin of the remaining two particles relative to the core. The hyperspherical method was used here to convert two-dimensional partial differential equation into a set of coupled one-dimensional equations. The Jacobi coordinates (x, y) are transformed into the hyperspherical coordinates (hyper-radius ρ and hyper-angle θ) defined as

$$\rho^2 = x^2 + y^2 \quad \text{and} \quad \theta = \arctan\left(\frac{x}{y}\right).$$

The hyperspherical expansion of the three-body radial and angular wave functions is

$$R_n(\rho) = \frac{\rho^{\frac{5}{2}}}{\rho_o^3}\sqrt{\frac{n!}{(n+5)!}}L^5_{n\,\text{lag}}(z)\exp\left(\frac{-z}{2}\right), \tag{3}$$

where $z = \rho/\rho_o$.

$$\psi_k^{l_x l_y}(\theta) = N_k^{l_x l_y}(\sin\theta)^{l_x}(\cos\theta)^{ly}P_n^{l_x+\frac{1}{2},l_y+\frac{1}{2}}(\cos 2\theta)\,. \tag{4}$$

The wave function of the valence neutrons is

$$\psi_{n,k}^{l_x l_y}(\rho, \theta) = R_n(\rho)\psi_k^{l_x l_y}(\theta)\,. \tag{5}$$

So $\psi(x, y)$ in Eq. (2) is

$$\psi(x, y) = \psi_{n,k}^{l_x l_y}(\rho, \theta)\,,$$

where $L^5_{n\,\text{lag}}(z)$ are Associated Laguerre Polynomials of the $n\,\text{lag} = 0, 1, 2, \ldots,$ $P_n^{l_x+\frac{1}{2},l_y+\frac{1}{2}}(\cos 2\theta)$ is the Jacobi Polynomial. Equation (3) is function of (ρ) because of the z dependence on (ρ) with $z = \rho/\rho_o$. Values of ρ and ρ_o are explained in Sec. 3. $n = l_x + 1$ and we assumed $n\,\text{lag} = n$. $N_k^{l_x l_y}$ is a normalization coefficient and k is the hyperangular momentum quantum number $k = l_x + l_y + 2n$ for $(n = 0, 1, 2, \ldots)$. The wave function of the system comes from the internal wave function of every body in that system. The internal wave function of each neutron were obtained by solving the Schrödinger equation in spherical coordinates. More details about the formalism of the hyperspherical harmonics method is presented in Refs. 41 and 42. The total Hamiltonian $\hat{H}$, of the system is

$$\hat{H} = \hat{T} + \hat{h}_{\text{core}}(\boldsymbol{\xi}) + \hat{V}_{\text{core-}n1}(r_{\text{core-}n1}, \boldsymbol{\xi}) + \hat{V}_{\text{core-}n2}(r_{\text{core-}n2}, \boldsymbol{\xi}) + \hat{V}_{n-n}(r_{n-n})\,. \tag{6}$$

The Hamiltonian contains the kinetic energy $\hat{T} = \hat{T}_x + \hat{T}_y$, the intrinsic Hamiltonian of the core $\hat{h}_{\text{core}}(\boldsymbol{\xi})$ which depends on the internal variables $\boldsymbol{\xi}$, a two-body interaction $V_{\text{core-}n}$ and V_{n-n} are for all pairs of interacting bodies. Here the potential is taken as a deformed Wood–Saxon potential as well as a spin–orbit interaction.

The rotational model is assumed for the structure of the core, hence the core is a deformed axially symmetric rotor, in the body-fixed frame the radius of this deformed core is expanded in spherical harmonic and, for simplicity, we retain only the quadrupole term, as Eq. (9).

$$\hat{V}_{\text{core-}n}(r_{\text{core-}n}, \boldsymbol{\xi}) = \frac{-V_0}{\left[1 + \exp\left(\dfrac{r_{\text{core-}n} - R(\theta,\phi)}{a}\right)\right]} + \frac{-\hbar^2}{m^2c^2}(2l \cdot s)\frac{V_{\text{so}}}{4r_{\text{core-}n}}\frac{d}{dr_{\text{core-}n}}\left(\left[1 + \exp\left(\frac{r_{\text{core-}n} - R_{\text{so}}}{a_{\text{so}}}\right)^{-1}\right]\right), \tag{7}$$

$$V_{n-n}(r_{n-n}) = -\frac{\hbar^2}{m^2c^2}(2l \cdot s)\frac{V_{\text{so}}}{4r_{n-n}}\frac{d}{dr_{n-n}}\left(\left[1 + \exp\left(\frac{r_{n-n} - R_{\text{so}}}{a_{\text{so}}}\right)^{-1}\right]\right), \tag{8}$$

with

$$R = R_0[1 + \beta_2 Y_{20}(\theta, \phi)]\,. \tag{9}$$

$R_0 = 1.25\, A_{\text{core}}^{\frac{1}{3}}$, we assumed $R_{\text{so}} = R$ and l is the operator of orbital momentum between core and a neutron, $\mathbf{s}$ is the operator of a neutron's spin and $m = m_\pi$ is the mass of pion for practical calculations $(\frac{\hbar}{m_\pi}) = 2.0$ fm^2, β_2 is the core's quadrupole deformation and A_{core} is the mass number of the core. The operator for the average squared distance of nucleons for an A-body system from the position of total center of mass

$$\mathbf{r}_{\text{CM}} = \frac{1}{A}\sum_{i=1}^{A}\mathbf{r}_i\,, \tag{10}$$

$$r_m^2 = \frac{1}{A}\sum_{i=1}^{A}(\mathbf{r}_i - \mathbf{r}_{\text{CM}})^2\,, \tag{11}$$

where r_i is the position of i nucleon, r_{CM} is center of mass and the rms matter radius $\langle r_m^2\rangle^{\frac{1}{2}}$ of the nucleus is

$$\langle r_m^2\rangle^{\frac{1}{2}} = \frac{1}{A}[A_{\text{core}}\langle r_m^2(\text{core}\rangle + \langle\rho^2\rangle)]\,. \tag{12}$$

The total quadrupole moment for halo nuclei can be written as $Q = Q_j + Q_c$, Q is the total quadrupole moment composed of Q_j due to the loose nucleon and Q_c due to the core. Generally $Q_c \gg Q_j$.[43]

$$Q_c = Q'\left[(3\Omega^2/2J^2) - \frac{1}{2}\right]. \tag{13}$$

Equation (13) can be written as

$$Q_c = Q' \frac{J}{2J+3}\left[\frac{3\Omega^2}{J(J+1)} - 1\right], \tag{14}$$

where J is the total nuclear angular momentum, Ω is the projection of j (nuclear angular momentum) and Q' can be taken equal to

$$Q' = \frac{4}{5}\delta Z R^2,$$

where Z is atomic number, R radius of the nucleus calculated before and δ is related to the deformation parameter β_2 ($\beta_2 = 2/3(4\pi/5)^{1/2}\delta$).[43]

3. Calculation Method and Results

In Fig. 2, the three bodies are the core and two neutrons with the wave function of each particle, as explained in the figure and described in the theoretical section. Equation (5) describes a wave function of the valence neutrons, ϕ in Eq. (2) describes a wave function of the core, calculated by using shell model and Eq. (2) itself describe a total wave function of three-body system.

The three-body Hamiltonian, Eq. (6) has been applied to calculate energy of two-neutron halo nucleus. The relationship between the three-body depends on the central Wood–Saxon potential and spin–orbit interaction as in Eq. (7). The two configurations (T-configuration and Y-configuration) were used in the calculation by using Jacobi coordinates. With assumption that the core is deformed and is connected to the two neutrons. The bounded states energies of ^{11}Li, the binding energy, the matter rms radius and a deformation of ^{9}Li were calculated. The values of ρ and ρ_o in Eq. (3) were approximated from the formulas

$$\rho_o = \sqrt{j(j+1)}, \quad \text{where} \quad j = l_x + \frac{1}{2},$$

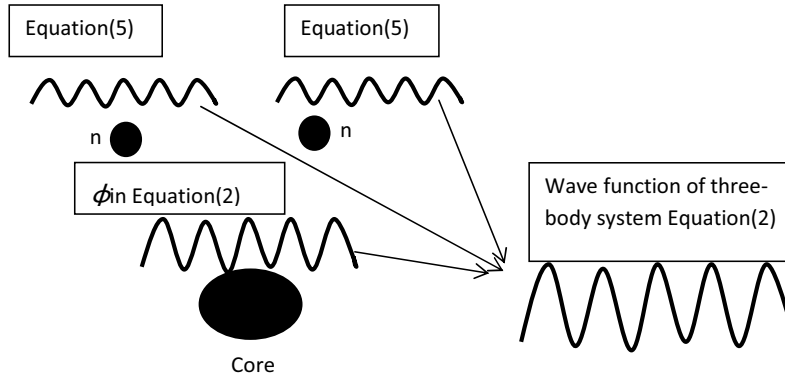

Fig. 2. Description of wave functions of three-body nucleus.

$$\rho = \sqrt{m_j(m_j+1)}, \quad \text{where} \;\; m_j = -j, -j+1, \ldots, j\,,$$

where the total angular momentum (j) of the valence neutron depends on the radius of core-n, so using these approximations, ρ and ρ_o were calculated.

In Eq. (9), $Y_{20}(\theta,\phi)$ is taken as

$$Y_{20}(\theta,\phi) = \frac{1}{4}\sqrt{\frac{5}{\pi}}(3\cos^2(\theta)-1)\,.$$

The central Wood–Saxon depends on the core's quadrupole deformation parameter β_2 through the radius R, Eq. (9). Throughout the present work, the spin–orbit term was left deformed (with radius $r_o = 1.25$ fm where $R_o = r_o A^{1/3}$). Radius $R_{\rm so}$ was made equal to R at all deformation. The diffuseness was fixed to the standard value $a_{\rm ws} = a_{\rm so} = 0.65$ fm. The calculations were performed for the full range of the deformation parameter $\beta_2 \in [-0.7, 0.7]$. The properties of ^{11}Li has been calculated upon variation of the core deformation β_2 with fix spin–orbit depth, $V_{\rm so}$ at 7.5 MeV and the central Wood–Saxon depth, V_o at 74 MeV.

Table 1 contains all the parameters used in the calculations. To determine the properties of three-body halo nuclei for ^{11}Li, the properties of two-body system of ^{10}Li treated as the ground state for ^{11}Li must be understood. The information about ^{10}Li is that, the ^{10}Li nucleus consist of a core and valence neutron placed in a $2s_{1/2}$ state with energy about 50 keV, $1p_{1/2}$ resonant state or p-resonance is assumed to be about 500 keV[28] and no evidence for a d-state, so will be considered the d-resonance. Figure 3 shows the variation of potential with deformation, where the core-n potentials have been effected by core deformation. The core-n potential increases as β_2 increases (for $\beta_2 > 0$) and the nucleus has a prolate shape. This influence the position of two-body energy state of ^{10}Li as shown in Fig. 4. Note that, the ground state of the core ^{9}Li is $J^\pi(^9\text{Li}) = 3/2^-$. The valence neutron may be coupled to the ground state of the ^{9}Li core to produce a nuclear state $J^\pi(^{10}\text{Li})$ or the valence neutron may be coupled to the excited state of the ^{9}Li core. We can expect two $p_{1/2}$-resonances built on an inert core $[1p_{1/2} \otimes 0^+]1/2^+$ and on the excited core $[1d_{5/2} \otimes 2^+]1/2^+$. From Fig. 4, the unbound energy is at higher deformation on the negative side (oblate shape) at $\beta_2 < -0.4$. Also shown in Fig. 4,

Table 1. Parameters of calculations.

l_x	l_y	n	K	ρ	ρ_o	r_o (fm)	a (fm)	$a_{\rm so}$ (fm)	V_o (MeV)	$V_{\rm so}$ (MeV)
0	0	1	2	0.866	0.866	1.25	0.65	0.65	−74	−7.5
1	1	2	6	0.866	1.936	1.25	0.65	0.65	−74	−7.5
—	—	—	—	1.936	—	1.25	0.65	—	—	—
2	2	3	10	0.866	2.958	1.25	0.65	—	—	—
2	2	3	10	1.936	—	1.25	—	—	—	—
2	—	—	—	2.958	—	1.25	—	—	—	—

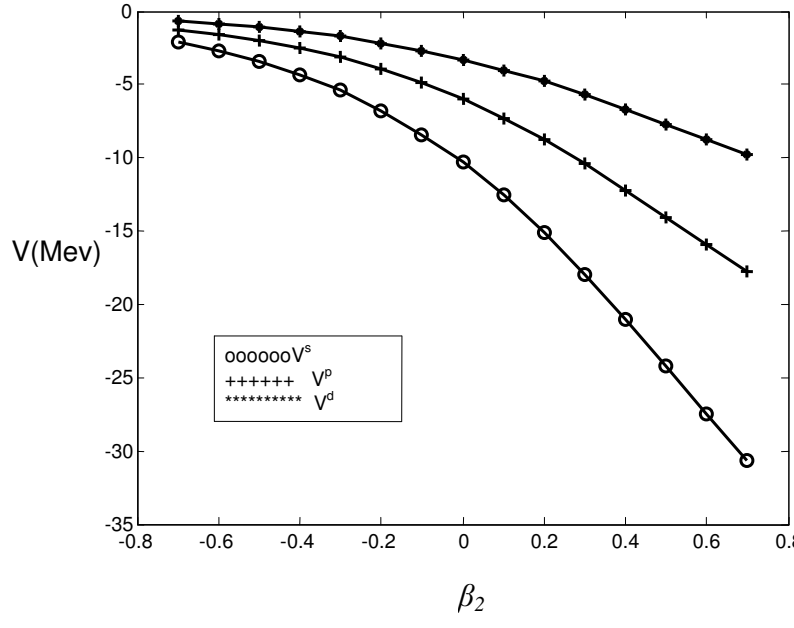

Fig. 3. ^{9}Li-n potential as function of deformation.

the second component disappear, suggesting that a neutron built on an excited core is not entirely accurate.

In the present work, the binding energy, matter radius of the three-body system (^{11}Li) and deformation of the core (^{9}Li) were calculated with normalization and using experimental data. The deformation of the core plays a big role and has high influence on the two-neutron halo nucleus of ^{11}Li. Depending on the relationship between deformation of the core and properties of two-neutron halo nucleus, these properties have been calculated. The experimental data for the above properties are given in Table 2.

Figure 5 describes variation of binding energy of three-body system with core deformation. Two configurations have been shown in Fig. 5. The differences between two configurations are not big, indicating that the spin–orbit interaction does not have a large effect comparison to the central potential effect. The variation of matter radius of three-body system with deformation is given in Fig, 6. As shown in Figs. 5 and 6 the properties of three-body system depended on the deformation of a core.

The normalization method was used to determine the above properties. The experimental value of deformation parameter of ^{9}Li ($\beta_2 = -0.2$) from Table 2 has been used both in Fig. 5 to obtain value of binding energy of three-body system ^{11}Li, and also in Fig. 6. To get value of matter radius of two-neutron halo nucleus ^{11}Li. All these values are given in Table 3.

The latest value of experimental data for the matter radius of ^{11}Li ($R_m^{\exp} = 3.12$ fm) was used to calculate the deformation of the core ^{9}Li and binding energy

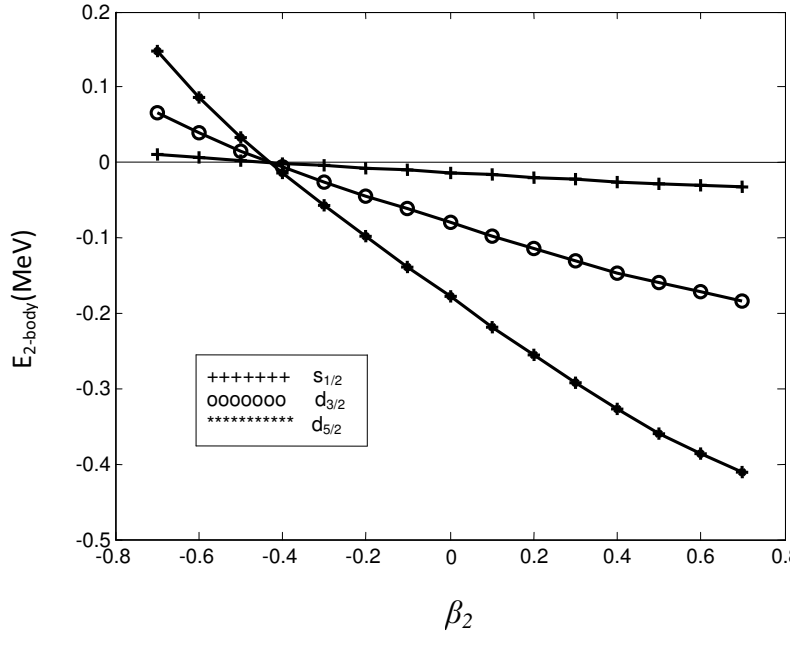

Fig. 4. Energy of bound state in ^{10}Li as function of deformation with ground state of the core $(^9\text{Li})p^-_{3/2}$.

Table 2. Experimental data of binding energy, matter radius of ^{11}Li and quadrupole moment of ^{9}Li.

Nucleus	E_{exp} (keV)[44,11]	R_m^{exp} (fm)[45–47]	Quadrupole (mb)[48]
^{11}Li	$-369.15(65)$	3.27 ± 0.24	
—	-378 ± 5	3.12 ± 0.66	
—		3.55 ± 0.1	
^{9}Li			$-30.6(2)$ ($\beta_2 = -0.2$)

of ^{11}Li nucleus. This value has been used in Fig. 6, the deformation parameter of ^{9}Li, was obtained about ($\beta_2 = -0.195$) and this was used to determine the binding energy from Fig. 5, as shown in Table 4.

Similarly, as above, the experimental data for binding energy of ^{11}Li ($E^{\text{exp}} = -369.15(65)$ keV) has been used in Fig. 5 to determine value of core deformation and then this value (of β_2, deformation parameter of the ^{9}Li core) was used in Fig. 6 to calculate matter radius of ^{11}Li, which was found to be about (2.6 fm), as shown in Fig. 6 and also given in Table 5. On the figure both experimental data and theoretical are in agreement that ^{9}Li nucleus is deformed (oblate) but with a bigger deformation parameter theoretically, and rms of about 2.6 fm.

Figure 7 shows the probabilities of the main components of three-body wave function $(s_{1/2})^2$, $(p_{1/2})^2$ and $(d_{5/2})^2$. The β_2 dependence of these probabilities has

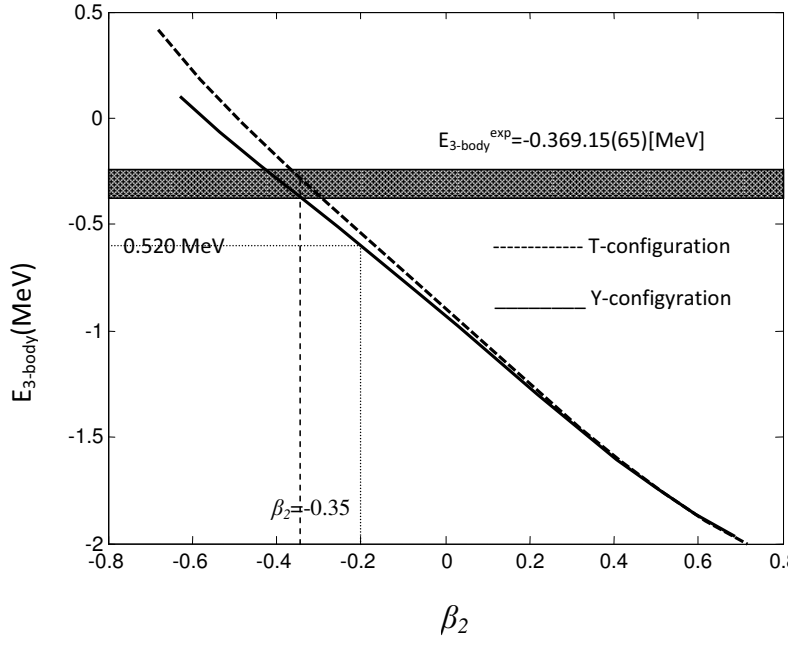

Fig. 5. Energy of bound state in ^{11}Li as function of deformation with ground state of the core $(^{9}\mathrm{Li})\rho^{-}_{3/2}$.

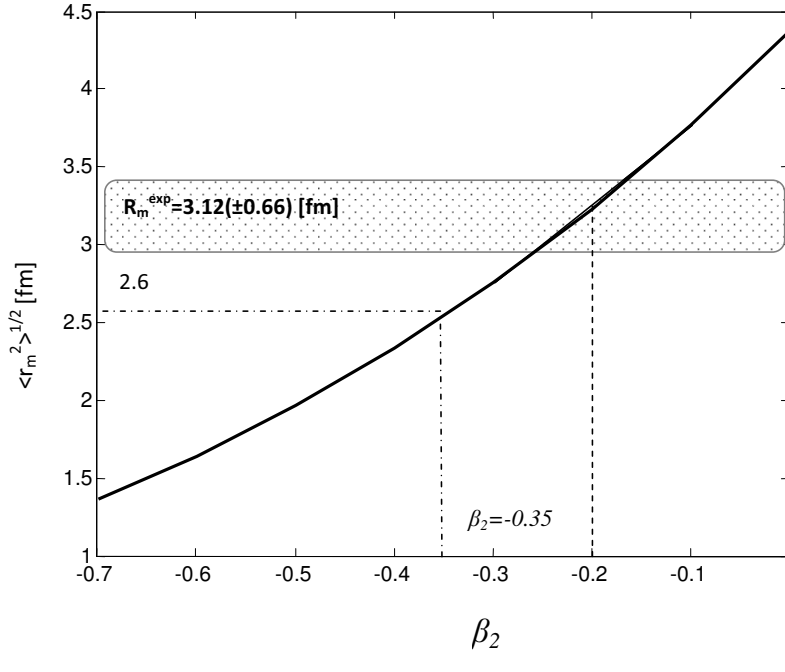

Fig. 6. Rms matter radius of ^{11}Li as a function of deformation.

Table 3. Experimental value of quadrupole moment of ^{9}Li with theoretical value (calculated) of binding energy and matter radius of ^{11}Li.

Nucleus	Quadrupole (mb) exp.	Binding energy (keV) calculated	Matter radius (fm) calculated
^{9}Li	$-30.6(2)$ ($\beta_2 = -0.2$)[48]		
^{11}Li		-520	3.25

Table 4. Experimental value of matter radius of ^{11}Li with theoretical value (calculated) of binding energy of ^{11}Li and deformation parameter of ^{9}Li.

Nucleus	Matter radius (fm) exp.	Deformation parameter (β_2) calculated	Binding energy (keV) calculated
^{11}Li	3.12[46]		-530
^{9}Li		-0.195	

Table 5. Experimental value of binding energy of ^{11}Li with theoretical value (calculated) of matter radius of ^{11}Li and deformation parameter of ^{9}Li.

Nucleus	Binding energy (keV) exp.	Deformation parameter (β_2) calculated	Matter radius (fm) calculated
^{11}Li	$-369.15(65)$[44]		2.6
^{9}Li		-0.35	

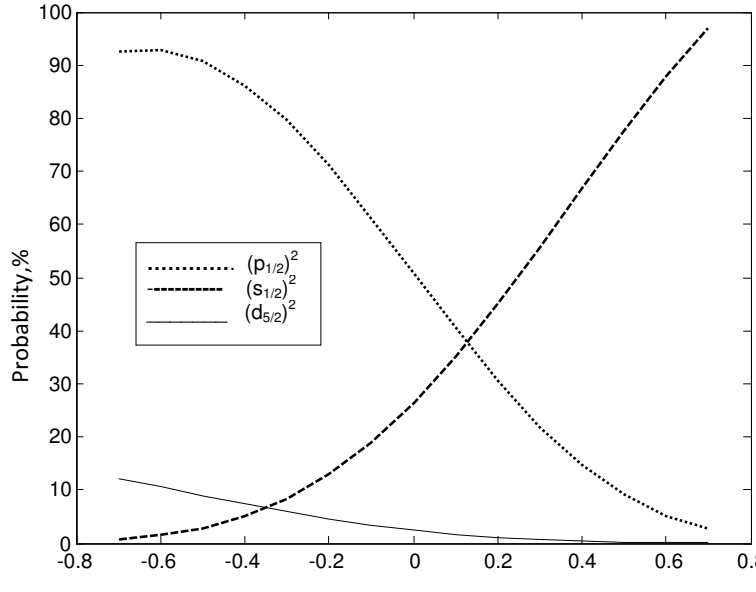

Fig. 7. Probabilities of the main components in the three-body wave function of ^{11}Li as a function of β_2.

been studied for fixed V_o and V_{ls}. From Fig. 7, for high deformation (oblate shape), the $(p_{1/2})^2$ probability is more than 90% and decreases quickly with β_2, while for high deformation but (prolate shape), the $(s_{1/2})^2$ probability is more than 90%. The $(s_{1/2})^2$ component increases with positive β_2, where on the whole the contribution of the $(d_{5/2})^2$ is small which is about 10% when $\beta_2 = -0.7$ and decreases with β_2. The $(p_{1/2})^2$ and $(s_{1/2})^2$ components were 70% and 14%, respectively for the experimental value of β_2 ($\beta_2 = -0.2$). In general the contribution of the components as shown in Fig. 7, are in agreement with that obtained in Ref. 5, but with some contrasting values, especially for the $(p_{1/2})^2$ and $(s_{1/2})^2$ components, while in full agreement with $(d_{5/2})^2$ component.

4. Conclusion

In the present work, a cluster model calculation was performed to determine the properties of nuclear structure for the two-neutron halo nucleus of ^{11}Li. Our calculation for a three-body problem has treated ^{11}Li as a core + n + n with the core, considered deformed and the calculated effect that deformation on two-body and three-body energies. The calculations have been performed base on Jacobi coordinates for two configurations T-configuration and Y-configuration to describe two-neutron halo nucleus of ^{11}Li. The two-body system of ^{10}Li throughout this work has been confirmed as an unbound system and consequently the ^{11}Li nucleus has Borromean property. Through normalization and the using of experimental data, the binding energy, matter radius of ^{11}Li nucleus and also deformation of ^{9}Li were calculated. The dependence on this method of calculation has shown that the core is deformed (oblate shape). This deformation has a clear effect on the bound state of the two-body and three-body system. The loosely bound state of the last two neutrons and the large matter radius of ^{11}Li nucleus have been confirmed in this work.

Acknowledgment

The authors would like to acknowledge the financial support from the Ministry of Higher Education Malaysia and University Kebangsaan Malaysia (through the Exploratory Research Grant Scheme) ERGS/1/2011/STG/UKM/02/64.

The authors would also like to thank Prof. I. J. Thompson from University of Surrey for the useful guidance.

References

1. I. Tanihata *et al.*, *Phys. Lett. B* **206** (1988) 592.
2. W. Mittig *et al.*, *Phys. Rev. Lett.* **59** (1987) 1889.
3. M. G. Saint-Laurent *et al.*, *Z. Phys. A* **332** (1989) 457.
4. P. Hansen and B. Jonson, *Europhys. Lett.* **4** (1987) 409.
5. Ivan Brida, A microscopic hyperspherical model of two-neutron halo nuclei, Ph.D. thesis, Michigan State University, USA (2009).

6. A. M. Poskanzer *et al.*, *Phys. Rev. Lett.* **17** (1966) 1271.
7. I. Tanihata *et al.*, *Phys. Lett. B* **160** (1985) 380.
8. T. Kobayashi *et al.*, *Phys. Rev. Lett.* **60** (1988) 2599.
9. B. M. Young *et al.*, *Phys. Rev. Lett.* **71** (1993) 4124.
10. C. Bachelet *et al.*, *Eur. Phys. J. A* **25** (2005) sl.31.
11. C. Bachelet *et al.*, *Phys. Rev. Lett.* **100** (2008) 182501.
12. T. Kobayashi *et al.*, *Phys. Lett. B* **232** (1989) 51.
13. R. Anne *et al.*, *Phys. Lett. B* **250** (1990) 19.
14. B. Blank *et al.*, *Z. Phys. A* **340** (1991) 41.
15. I. Tanihata *et al.*, *Phys. Lett. B* **287** (1992) 307.
16. C.-B. Moon *et al.*, *Phys. Lett. B* **297** (1992) 39.
17. I. Mukha *et al.*, *Phys. Lett. B* **367** (1996) 65.
18. M. J. G. Borge *et al.*, *Nucl. Phys. A* **613** (1997) 199.
19. R. Raabe *et al.*, *Phys. Rev. Lett.* **101** (2008) 212501.
20. I. Tanihata, *J. Phys. G: Nucl. Part. Phys.* **22** (1996) 157.
21. I. J. Thompson, *Nucl. Phys. A* **701** (2002) 7.
22. N. Keeley *et al.*, *Prog. Part. Nucl. Phys.* **59** (2007) 579.
23. M. Smith *et al.*, arXiv:0807.1260v2 [nucl-ex] (2008).
24. R. Sanchez *et al.*, *Phys. Rev. Lett.* **96** (2006) 033002.
25. R. Neugart *et al.*, *Phys. Rev. Lett.* **101** (2008) 132502.
26. M. V. Zhukov *et al.*, *Phys. Rep.* **231** (1993) 151.
27. J. M. Bang and I. J. Thompson, *Phys. Lett. B* **279** (1992) 201.
28. E. Garrido, D. V. Fedorov and A. S. Jensen, *Nucl. Phys. A* **700** (2002) 117.
29. M. V. Zhukov *et al.*, *Phys. Lett. B* **265** (1991) 19.
30. L. Johannsen, A. S. Jensen and P. G. Hansen, *Phys. Lett. B* **244** (1990) 357.
31. G. F. Bertsch and H. Esbensen, *Ann. Phys.* **209** (1991) 327.
32. Y. Tosaka and Y. Suzuki, *Nucl. Phys. A* **512** (1990) 46.
33. K. Ikeda, *Nucl. Phys. A* **538** (1992) 355c.
34. N. Vinh Mau and J. C. Pacheco, *Nucl. Phys. A* **607** (1996) 163.
35. F. M. Nunes, Core excitation in few-body systems: Application to light exotic nuclei, Ph.D. thesis, University of Surrey, England, 1995.
36. B. R. Barrett *et al.*, *Nucl. Phys. A* **746** (2004) 579.
37. P. Navratil and B. R. Barrett, *Phys. Rev. C* **57** (1998) 3119.
38. K. Varga and Y. Suzuki, *Phys. Rev. C* **52** (1995) 2885.
39. K. Arai *et al.*, *Prog. Theor. Phys. Suppl.* **142** (2001) 97.
40. K. Varga, Y. Suzuki and R. G. Lovas, *Phys. Rev. C* **66** (2002) 041302.
41. F. M. Nunes, J. A. Christley, I. J. Thompson, R. C. Johnson and V. D. Efros, *Nucl. Phys. A* **609** (1996) 43.
42. T. Tarutina and I. J. Thompson, *Nucl. Phys. A* **733** (2004) 53.
43. W. E. Hornyak, Nuclear Structure Book, 1975.
44. M. Smith, M. Brodeur and T. Brunner *et al.*, *Phys. Rev. Lett.* **101** (2008) 202501.
45. I. Tanihata and H. Hamagaki *et al.*, *Phys. Rev. Lett.* **55** (1985) 2676.
46. A. Ozawa, T. Suzuki and I. Tanihata, *Nucl. Phys. A* **693** (2001) 32.
47. J. S. Al-Khalili and J. A. Tostevin, *Phys. Rev. Lett.* **76** (1996) 3903.
48. W. Nortershauser and T. Neff, *Phys. Rev. C* **84** (2011) 024307.